

Phase diagram and thermodynamics of the PNJL model*

Claudia Ratti^{a,b}, Michael A. Thaler^a and Wolfram Weise^a

^aPhysik-Department, Technische Universität München, D-85747 Garching, Germany

^bECT*, I-38050 Villazzano (Trento), Italy

and INFN, Gruppo Collegato di Trento, Via Sommarive, 38050 POVO

October 15, 2018

Abstract

QCD-based thermodynamics at zero and finite quark chemical potential is studied using an extended Nambu and Jona-Lasinio approach in which quarks couple simultaneously to the chiral condensate and to a background temporal gauge field representing Polyakov loop dynamics. This so-called PNJL model thus includes features of both deconfinement and chiral symmetry restoration. We discuss the phase diagram as it emerges from this approach in close comparison with results from lattice QCD thermodynamics. The critical point, separating crossover from first order phase transition, is investigated with special focus on its quark mass dependence, starting from the relatively large masses presently accessible by lattice simulations, down to the chiral limit.

1 Introduction and Basics

Models of the Nambu and Jona-Lasinio (NJL) type [1] have a long history and have been used extensively to describe the dynamics and thermodynamics of the lightest hadrons [2–5], including investigations of phase diagrams [6, 7]. Such schematic models offer a simple and practical illustration of the basic mechanisms that drive spontaneous chiral symmetry breaking, a key feature of QCD in its low-temperature, low-density phase.

The NJL model is based on an effective Lagrangian of relativistic fermions (quarks) which interact through local current-current couplings, assuming that gluonic degrees of freedom can be frozen into pointlike effective interactions between

*Work supported in part by BMBF and GSI

quarks. Lattice QCD results for the gluonic field strength correlation function [9] demonstrate that the colour correlation length, i.e. the distance over which colour fields propagate in the QCD vacuum, is small, of order 0.2 fm corresponding to a characteristic momentum scale Λ of order 1 GeV. Consider now the basic non-local interaction between two quark colour currents, $J_i^\mu = \bar{\psi}\gamma^\mu t_i\psi$, where t_i are the generators of the $SU(N_c)$ colour gauge group. The contribution of this current-current coupling to the action is:

$$S_{int} = -\frac{1}{2} \int d^4x d^4y J_i^\mu(x) g^2 D_{\mu\nu}^{ij}(x, y) J_j^\mu(y) \quad , \quad (1)$$

where $D_{\mu\nu}^{ij}$ is the full gluon propagator and g is the QCD coupling. In perturbative QCD this S_{int} generates the familiar one-gluon exchange interaction between quarks and maintains its non-local structure. That is the situation realised in the quark-gluon phase at extremely high temperatures. As one approaches the hadronic phase around a critical temperature of about 0.2 GeV, the propagating gluons experience strong screening effects which cannot be handled perturbatively. If the range over which colour can be transported is now restricted to the short distance scale Λ^{-1} , while typical momentum scales (Fermi momenta) of the quarks are small compared to Λ , then the quarks experience an interaction which can be approximated by a local coupling between their colour currents:

$$\mathcal{L}_{int} = -G_c J_\mu^i(x) J_i^\mu(x) \quad , \quad (2)$$

where $G_c \sim \bar{g}^2 \Lambda^{-2}$ is an effective coupling strength of dimension $length^2$ which encodes the QCD coupling, averaged over the relevant distance scales, in combination with the squared correlation length, Λ^{-2} . In essence, by “integrating out” gluon degrees of freedom and absorbing them in the four-fermion interaction \mathcal{L}_{int} , the local $SU(N_c)$ gauge symmetry of QCD is now replaced by a global $SU(N_c)$ symmetry of the NJL model. Apart from this step, the interaction Lagrangian (2) evidently preserves the chiral $SU(N_f) \times SU(N_f)$ symmetry that it shares with the original QCD Lagrangian for N_f massless quark flavours.

A Fierz transform of the colour current-current interaction (2) produces a set of exchange terms acting in quark-antiquark channels. For the $N_f = 2$ case:

$$\mathcal{L}_{int} \rightarrow \frac{G}{2} [(\bar{\psi}\psi)^2 + (\bar{\psi}i\gamma_5\vec{\tau}\psi)^2] + \dots \quad , \quad (3)$$

where $\vec{\tau} = (\tau_1, \tau_2, \tau_3)$ are the isospin $SU(2)$ Pauli matrices. Not shown for brevity is a series of terms with combinations of vector and axial vector currents, both in colour singlet and colour octet channels. The constant G is proportional to the colour coupling strength G_c . Their ratio is uniquely determined by N_c and N_f .

Eq.(3) is the starting point of the standard NJL model. In the mean field (Hartree) approximation, the NJL equation of motion leads to the gap equation

$$m = m_0 - G\langle\bar{\psi}\psi\rangle . \quad (4)$$

With a small bare (current) quark mass m_0 as input, this equation links the dynamical generation of a large constituent quark mass m to spontaneous chiral symmetry breaking and the appearance of the quark condensate

$$\langle\bar{\psi}\psi\rangle = -Tr \lim_{x \rightarrow 0^+} \langle\mathcal{T}\psi(0)\bar{\psi}(x)\rangle = -2iN_f N_c \int \frac{d^4p}{(2\pi)^4} \frac{m \theta(\Lambda^2 - \vec{p}^2)}{p^2 - m^2 + i\varepsilon} . \quad (5)$$

For $m_0 = 0$ a non-zero quasiparticle mass develops dynamically, together with a non-vanishing chiral condensate, once G exceeds a critical value. The procedure requires a momentum cutoff $\Lambda \simeq 2m$ beyond which the interaction is “turned off”. Note that the strong interaction, by polarizing the vacuum and turning it into a condensate of quark-antiquark pairs, transforms an initially pointlike quark with its small bare mass m_0 into a massive quasiparticle with a finite size. (Such an NJL-type mechanism is commonly thought to be at the origin of the phenomenological constituent quark masses $m \sim 0.3\text{-}0.4$ GeV).

While the NJL model illustrates the transmutation of originally light (or even massless) quarks and antiquarks into massive quasiparticles, it generates at the same time pions as Goldstone bosons of spontaneously broken chiral symmetry. NJL type approaches have also been used extensively to explore colour superconducting phases at high densities through the formation of various sorts of diquark condensates [6, 8].

Despite their widespread use, NJL models have a principal deficiency. The reduction to global (rather than local) colour symmetry has the consequence that quark confinement is missing. Confinement is the second key feature of low-energy QCD besides spontaneous chiral symmetry breaking. While confinement is a less significant aspect for $N_c = 2$ thermodynamics which can be described quite successfully using the simplest NJL approach [10], it figures prominently for $N_c = 3$ QCD. There have been ongoing discussions whether deconfinement and the restoration of chiral symmetry are directly connected in the sense that they appear at the same transition temperature T_c , as suggested by earlier lattice computations. In any case, as one approaches T_c from above, all versions of the “classic” NJL model encounter the problem that they operate with the “wrong” degrees of freedom. Quarks as coloured quasiparticles are incorrectly permitted to propagate over large distances even in the hadronic sector of the phase diagram. In contrast, confinement and spontaneous chiral symmetry breaking imply that QCD below T_c turns into a low-energy effective theory of weakly interacting Goldstone bosons (pions) with derivative couplings to colour-singlet hadrons (rather than quarks).

In the limit of infinitely heavy quarks, the deconfinement phase transition is characterized by spontaneous breaking of the $Z(3)$ center symmetry of QCD. The

corresponding order parameter is the thermal Wilson line, or Polyakov loop, winding around the imaginary time direction with periodic boundary conditions:

$$\phi(\vec{x}) = N_c^{-1} \text{Tr} \mathcal{P} \exp \left[i \int_0^\beta d\tau A_4(\vec{x}, \tau) \right], \quad (6)$$

with $\beta = 1/T$ the inverse temperature. Here $A_4 = iA^0$ is the temporal component of the Euclidean gauge field (\vec{A}, A_4) and \mathcal{P} denotes path ordering. In the presence of dynamical quarks the $Z(3)$ symmetry is explicitly broken. The Polyakov loop ceases to be a rigorous order parameter but still serves as an indicator of a rapid crossover towards deconfinement.

Recent developments have aimed at a synthesis of the NJL model with Polyakov loop dynamics. The principal idea is to introduce both the chiral condensate $\langle \bar{\psi}\psi \rangle$ and the Polyakov loop ϕ as classical, homogeneous fields which couple to the quarks according to rules dictated by the symmetries and symmetry breaking patterns of QCD, thus unifying aspects of confinement and chiral symmetry breaking. We refer to this combined scheme as the PNJL (Polyakov-loop-extended NJL) model. The present writeup is largely based on our previous ref.[11]. It reviews results of calculations as well as presenting an outlook for further steps to be pursued in close comparison with results from lattice QCD thermodynamics.

2 Introducing the PNJL model

Throughout this presentation we work with two flavours ($N_f = 2$) and specify the PNJL Lagrangian [11] as follows. Its basic ingredients are the Nambu and Jona-Lasinio type four-fermion contact term and the coupling to a (spatially constant) temporal background gauge field representing Polyakov loop dynamics:

$$\mathcal{L}_{PNJL} = \bar{\psi} (i\gamma_\mu D^\mu - \hat{m}_0) \psi + \frac{G}{2} \left[(\bar{\psi}\psi)^2 + (\bar{\psi}i\gamma_5\vec{\tau}\psi)^2 \right] - \mathcal{U}(\phi[A], \phi^*[A]; T), \quad (7)$$

where $\psi = (\psi_u, \psi_d)^T$ is the quark field,

$$D^\mu = \partial^\mu - iA^\mu \quad \text{and} \quad A^\mu = \delta_0^\mu A^0, \quad (8)$$

with $A^0 = -iA_4$. The gauge coupling g is conveniently absorbed in the definition of $A^\mu(x) = g\mathcal{A}_a^\mu(x)\frac{\lambda_a}{2}$ where \mathcal{A}_a^μ is the SU(3) gauge field and λ_a are the Gell-Mann matrices. The two-flavour current quark mass matrix is $\hat{m}_0 = \text{diag}(m_u, m_d)$ and we shall work in the isospin symmetric limit with $m_u = m_d \equiv m_0$. As previously mentioned, G is the coupling strength of the chirally symmetric four-fermion interaction.

The effective potential $\mathcal{U}(\phi, \phi^*; T)$ is expressed in terms of the traced Polyakov loop (6), reduced to our case of a constant Euclidean field A_4 :

$$\phi = \frac{1}{3} \text{Tr}_c \exp \left[\frac{iA_4}{T} \right] . \quad (9)$$

In a convenient gauge (the so-called Polyakov gauge), the Polyakov loop matrix can be given a diagonal representation [12].

The effective potential \mathcal{U} has the following general features. It must satisfy the $Z(3)$ center symmetry just like the pure gauge QCD Lagrangian. Furthermore, in accordance with lattice results for the behaviour of the Polyakov loop as a function of temperature T , the potential \mathcal{U} must have a single minimum at $\phi = 0$ at small T , while at high T it develops a second minimum which becomes the absolute minimum above a critical temperature T_0 . In the limit $T \rightarrow \infty$ we have $\phi \rightarrow 1$. The following general form is chosen for \mathcal{U} , including a ϕ^3 term which reflects the underlying $Z(3)$ symmetry:

$$\frac{\mathcal{U}(\phi, \phi^*; T)}{T^4} = -\frac{b_2(T)}{2} \phi^* \phi - \frac{b_3}{6} (\phi^3 + \phi^{*3}) + \frac{b_4}{4} (\phi^* \phi)^2 \quad (10)$$

with

$$b_2(T) = a_0 + a_1 \left(\frac{T_0}{T} \right) + a_2 \left(\frac{T_0}{T} \right)^2 + a_3 \left(\frac{T_0}{T} \right)^3 . \quad (11)$$

A precision fit of the coefficients a_i , b_i is performed to reproduce the pure-gauge lattice data.

There is a subtlety about the Polyakov loop field, ϕ , and its conjugate, ϕ^* , in the presence of quarks. At zero chemical potential we have $\phi = \phi^*$, i.e. the field ϕ is real, it serves as an order parameter for deconfinement and a mean-field calculation is straightforward. At non-zero quark chemical potential, $Z(3)$ symmetry is explicitly broken and ϕ differs from ϕ^* while their thermal expectation values $\langle \phi \rangle$ and $\langle \phi^* \rangle$ remain real [13]. A detailed analysis of the stationary points of the action under these conditions requires calculations beyond mean field which will be reported elsewhere [14]. We proceed here, as in [11], by introducing $\Phi \equiv \langle \phi \rangle$ and $\bar{\Phi} \equiv \langle \phi^* \rangle$ as new independent field variables which replace ϕ and ϕ^* in Eq.(10). This approximate prescription corresponds to a modified mean-field scheme which can account for the difference between Φ and $\bar{\Phi}$ in the presence of quarks. The more accurate treatment is under way.

Using standard bosonization techniques, we introduce the auxiliary bosonic fields σ and $\vec{\pi}$ for the scalar-isoscalar and pseudoscalar-isovector quark bilinears in Eq.(7). The expectation value of the σ field is directly related to the chiral condensate by $\langle \sigma \rangle = G \langle \bar{\psi} \psi \rangle$ and the gap equation becomes

$$m = m_0 - \langle \sigma \rangle . \quad (12)$$

a_0	a_1	a_2	a_3	b_3	b_4
6.75	-1.95	2.625	-7.44	0.75	7.5

Table 1: Parameter set used in [11] for the Polyakov loop potential (10, 11).

Note that $\langle\sigma\rangle$ is negative in our representation, and the chiral (quark) condensate is $\langle\bar{\psi}\psi\rangle = \langle\bar{\psi}_u\psi_u + \bar{\psi}_d\psi_d\rangle$.

Before passing to the actual calculations, we summarize basic assumptions behind Eq.(7) and comment on limitations to be kept in mind. The PNJL model reduces gluon dynamics to a) chiral point couplings between quarks, and b) a simple static background field representing the Polyakov loop. This picture can be expected to work only within a limited range of temperatures. At large T , transverse gluons are known to be thermodynamically active degrees of freedom, but they are ignored in the PNJL model. To what extent this model can reproduce lattice QCD thermodynamics is nonetheless a relevant question. We can assume that its range of applicability is, roughly, $T \leq (2 - 3)T_c$, based on the conclusion drawn in ref. [15] that transverse gluons start to contribute significantly for $T > 2.5T_c$.

3 Parameter fixing

The parameters of the Polyakov loop potential \mathcal{U} are fitted to reproduce the lattice data [16] for QCD thermodynamics in the pure gauge sector. Minimizing $\mathcal{U}(\Phi, \bar{\Phi}, T)$ one has $\Phi = \bar{\Phi}$ and the pressure of the pure-gauge system is evaluated as $p(T) = -\mathcal{U}(T)$ with $\Phi(T)$ determined at the minimum. The entropy and energy density are then obtained by means of the standard thermodynamic relations. Fig.1(a) shows the behaviour of the Polyakov loop as a function of temperature, while Fig.1(b) displays the corresponding (scaled) pressure, energy density and entropy density. The lattice data are reproduced extremely well using the ansatz (10,11), with parameters summarized in Table 1. The critical temperature T_0 for deconfinement appearing in Eq. (11) is fixed at $T_0 = 270$ MeV in the pure gauge sector.

The pure NJL model part of the Lagrangian (7) has the following parameters: the “bare” quark mass m_0 , a three-momentum cutoff Λ and the coupling strength G . We fix them by reproducing the known chiral physics in the hadronic sector at $T = 0$: the pion decay constant f_π , the chiral condensate $|\langle\bar{\psi}_u\psi_u\rangle|^{1/3}$ and the pion mass m_π are evaluated in the model and adjusted at their empirical values. The results are shown in Table 2.

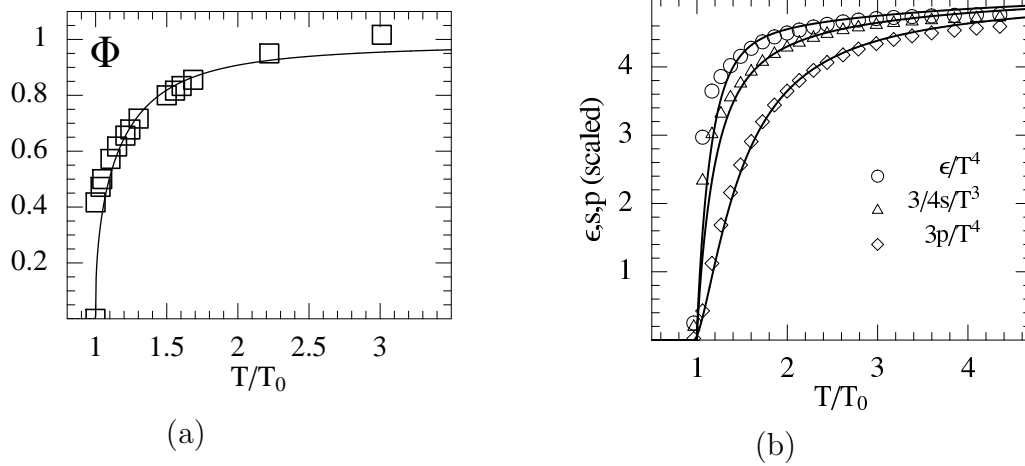


Figure 1: (a): Polyakov loop as a function of temperature in the pure gauge sector, compared to corresponding lattice results taken from Ref. [17]. (b): Scaled pressure, entropy density and energy density as functions of the temperature in the pure gauge sector, compared to the corresponding lattice data taken from Ref. [16].

Λ [GeV]	G [GeV ⁻²]	m_0 [MeV]
0.651	10.08	5.5
$ \langle\bar{\psi}_u\psi_u\rangle ^{1/3}$ [MeV]	f_π [MeV]	m_π [MeV]
251	92.3	139.3

Table 2: Parameter set used for the NJL model part of the effective Lagrangian (7), and the resulting physical quantities. These values of the parameters yield a constituent quark mass $m = 325$ MeV.

4 Finite μ thermodynamics

4.1 General features

We now extend the model to finite temperature and chemical potentials using the Matsubara formalism. We consider the isospin symmetric case, with an equal number of u and d quarks (and therefore a single quark chemical potential μ). The quantity to be minimized at finite temperature is the thermodynamic potential per unit volume:

$$\begin{aligned} \Omega &= \mathcal{U}(\Phi, \bar{\Phi}, T) + \frac{\sigma^2}{2G} \\ &- 2N_f T \int \frac{d^3p}{(2\pi)^3} \left\{ \text{Tr}_c \ln [1 + e^{-(E_p - \tilde{\mu})/T}] + \text{Tr}_c \ln [1 + e^{-(E_p + \tilde{\mu})/T}] \right\} \\ &- 6N_f \int \frac{d^3p}{(2\pi)^3} E_p \theta(\Lambda^2 - \vec{p}^2) \quad , \end{aligned} \quad (13)$$

where $\tilde{\mu} = \mu + iA_4$ and $E_p = \sqrt{\vec{p}^2 + m^2}$ is the quark quasiparticle energy. The last term involves the NJL three-momentum cutoff Λ . The second (finite) term does not require any cutoff.

Notice that the coupling of the Polyakov loop to quarks effectively reduces the residues at the quark quasiparticle poles as the critical temperature is approached from $T > T_c$: expanding the logarithms in the second line of (13) one finds $\text{Tr}_c \ln (1 + \exp[-(E_p - \mu - iA_4)/T]) = 3\phi \exp[-(E_p - \mu)/T] + \dots$, with ϕ then to be replaced by $\langle \phi \rangle \equiv \Phi$ which tends to zero as $T \rightarrow T_c$.

From the thermodynamic potential (13) the equations of motion for the mean fields σ, Φ and $\bar{\Phi}$ are determined through

$$\frac{\partial \Omega}{\partial \sigma} = 0, \quad \frac{\partial \Omega}{\partial \Phi} = 0, \quad \frac{\partial \Omega}{\partial \bar{\Phi}} = 0. \quad (14)$$

This set of coupled equations is then solved for the fields as functions of temperature T and quark chemical potential μ . Fig. 2(a) shows the chiral condensate together with the Polyakov loop Φ as functions of temperature at $\mu = 0$ where we find $\Phi = \bar{\Phi}$. One observes that the introduction of quarks coupled to the σ and Φ fields turns the first-order transition seen in pure-gauge lattice QCD into a continuous crossover. The crossover transitions for the chiral condensate $\langle \bar{\psi}\psi \rangle$ and for the Polyakov loop almost coincide at a critical temperature $T_c \simeq 220$ MeV (see Fig. 2(b)). We point out that this feature is obtained without changing a single parameter with respect to the pure gauge case. The value of the critical temperature found here is a little high if compared to the available data for two-flavour Lattice QCD [18] which give $T_c = (173 \pm 8)$ MeV. For quantitative comparison with existing lattice results we choose to reduce T_c by rescaling the parameter T_0 from 270 to 190 MeV. In this

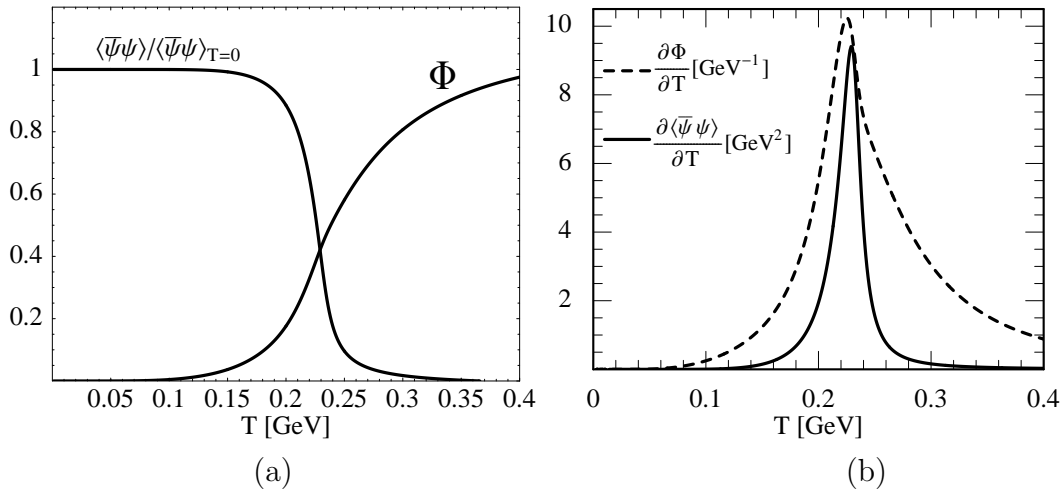


Figure 2: Left: scaled chiral condensate and Polyakov loop $\Phi(T)$ as functions of temperature at zero chemical potential. Right: plots of $\partial\langle\bar{\psi}\psi\rangle/\partial T$ and $\partial\Phi/\partial T$.

case we loose the perfect coincidence of the chiral and deconfinement transitions, but they are shifted relative to each other by less than 20 MeV. When defining T_c in this case as the average of the two transition temperatures we find $T_c = 180$ MeV.

4.2 Detailed comparison with lattice data

The primary aim is now to compare predictions of our PNJL model with the lattice data available for full QCD thermodynamics (with quarks included) at zero and finite chemical potential μ . Consider first the pressure $p(T, \mu = 0) = -\Omega(T, \mu = 0)$ of the quark-gluon system at zero chemical potential. Our results are presented in Fig. 3 in comparison with corresponding lattice data. We point out that the input parameters of the PNJL model have been fixed independently in the pure gauge and hadronic sectors, so that the calculated pressure is a prediction of the model, without any further tuning of parameters. With this in mind, the agreement with lattice results is quite satisfactory. Also shown in Fig. 3 is the result obtained in the standard NJL model. Its deficiencies are evident. At low temperatures the pressure comes out incorrect. The missing confinement permits quarks to be active degrees of freedom even in the forbidden region $T < T_c$. At high temperatures, the standard NJL result for the pressure is significantly lower than the one seen in the lattice data. The gluonic thermodynamics is missing altogether in the NJL model, whereas in the PNJL model it is partially taken into account by means of the Polyakov loop effective potential $\mathcal{U}(\Phi, \bar{\Phi}, T)$. As stated previously, the range of validity of this approach is limited, however, to temperatures smaller than $2.5 T_c$, beyond which transverse gluon degrees of freedom become important.

The introduction of the Polyakov loop within the PNJL quasiparticle model

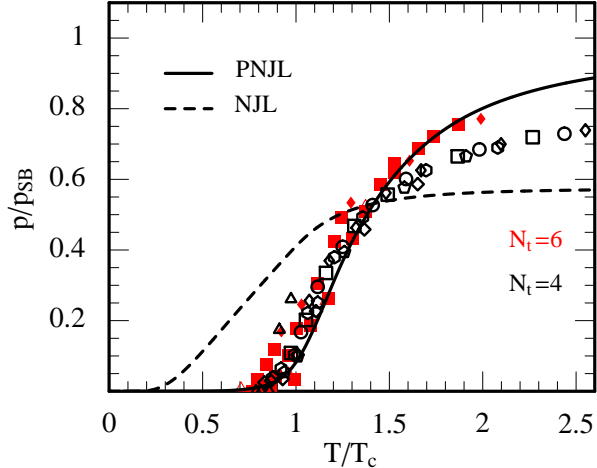


Figure 3: Scaled pressure divided by the Stefan-Boltzmann (ideal gas) limit as a function of temperature at zero chemical potential: comparison between our PNJL model prediction [11] (full line), the standard NJL model result (dashed) and lattice results corresponding to $N_t = 4$ and $N_t = 6$. Lattice data are taken from Ref. [19]

leads to a remarkable improvement in basically all thermodynamic quantities. The coupling of the quark quasiparticles to the field Φ reduces their weight as thermodynamically active degrees of freedom when the critical temperature T_c is approached from above. The quasiparticle exponentials $\exp[-(E_p \pm \mu)/T]$ are progressively suppressed in the thermodynamic potential as $T \rightarrow T_c$. This is what can be interpreted as the effect of confinement in the context of the PNJL model.

One must note that the lattice data are grouped in different sets obtained on lattices with temporal extent $N_t = 4$ and $N_t = 6$, both of which are not continuum extrapolated. In contrast, our calculation should, strictly speaking, be compared to the continuum limit. In order to perform meaningful comparisons, the pressure is divided by its asymptotic high-temperature (Stefan-Boltzmann) limit for each given case. At high temperatures our predicted curve should be located closer to the $N_t = 6$ set than to the one with $N_t = 4$. This is indeed the case.

At non-zero chemical potential, quantities of interest that have become accessible in lattice QCD are the “pressure difference” and the quark number density. The (scaled) pressure difference is defined as:

$$\frac{\Delta p(T, \mu)}{T^4} = \frac{p(T, \mu) - p(T, \mu = 0)}{T^4}. \quad (15)$$

A comparison of Δp , calculated in the PNJL model, with two-flavour lattice results is presented in Fig. 4. This figure shows the scaled pressure difference as a function of the temperature for a series of chemical potentials, with values ranging between $\mu = 0.2T_c^{(0)}$ and $\mu \simeq T_c^{(0)}$ where $T_c^{(0)} \equiv T_c(\mu = 0)$. The agreement between our results [11] and the lattice data is quite satisfactory.

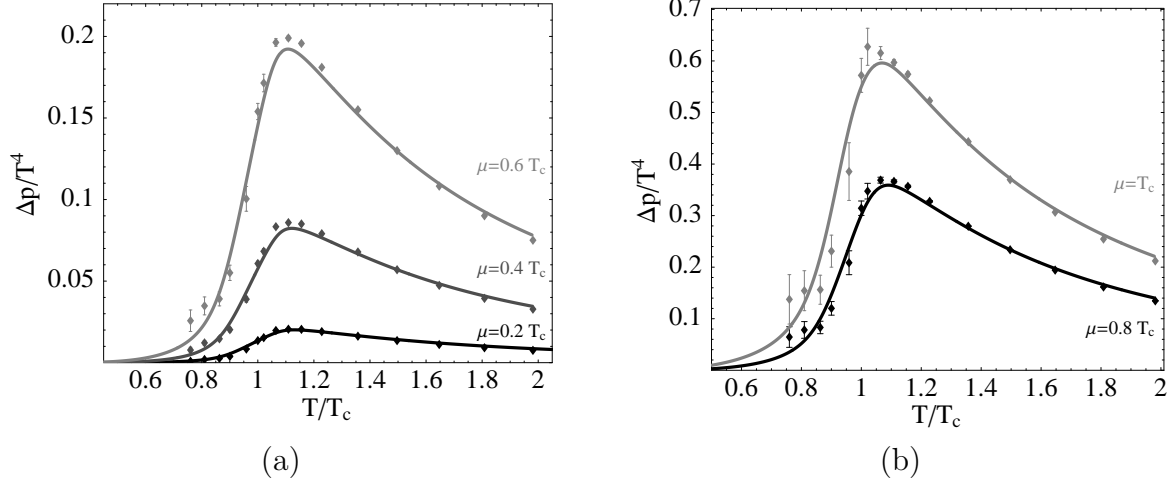


Figure 4: Scaled pressure difference as a function of temperature at different values of the quark chemical potential (results from Ref. [11]), compared to lattice data taken from Ref. [20].

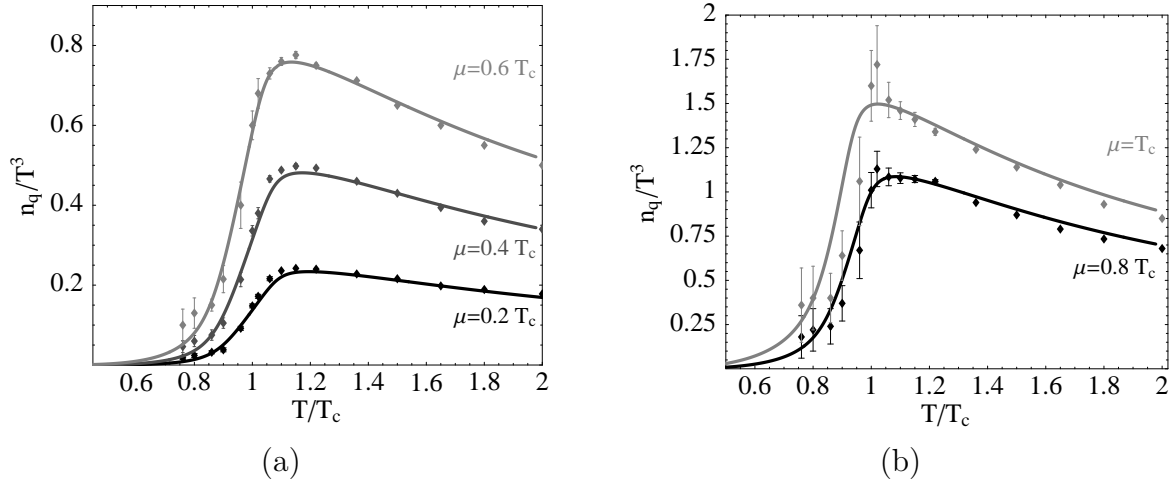


Figure 5: Scaled quark number densities [11] as a function of temperature at different values of the chemical potential, compared to lattice data taken from Ref. [20].

A related quantity for which lattice results at finite μ exist, is the scaled quark number density, defined as:

$$\frac{n_q(T, \mu)}{T^3} = -\frac{1}{T^3} \frac{\partial \Omega(T, \mu)}{\partial \mu}. \quad (16)$$

Results [11] for n_q as a function of the temperature, for different values of the quark chemical potential, are shown in Fig. 5 in comparison with corresponding lattice data [20]. Also in this case, the agreement between our PNJL model and the corresponding lattice data is surprisingly good.

It is a remarkable feature that the quark densities and the pressure difference at finite μ are so well reproduced even though the lattice “data” have been obtained by a Taylor expansion up to fourth order in μ , whereas our thermodynamical potential is used with its full functional dependence on μ . We have examined the convergence in powers of μ by expanding Eq. (13). It turns out that the Taylor expansion to order μ^2 deviates from the full result by less than 10 % even at a chemical potential as large as $\mu \sim T_c$. When expanded to $\mathcal{O}(\mu^4)$, no visible difference is left between the approximate and full calculations for all cases shown in Figs. 4 and 5.

An exact copy of our PNJL model [11] has recently been employed in [21] to calculate susceptibilities and higher order derivatives in the expansion of the pressure $p(T, \mu) = -\Omega(T, \mu)$ around $\mu = 0$.

$$\frac{p(T, \mu)}{T^4} = \sum_{n \text{ even}} c_n(T) \left(\frac{\mu}{T}\right)^n. \quad (17)$$

The resulting quark number susceptibility

$$c_2(T) = \frac{1}{2T^2} \left(\frac{\partial^2 p}{\partial \mu^2} \right)_{\mu=0} \quad (18)$$

compares well with lattice QCD computations. The higher-order coefficients $c_{4,6}$ reproduce the corresponding lattice data around T_c very well, but c_4 as obtained in the PNJL calculation tends to be too large at higher temperatures. For a more quantitative understanding, further steps are yet necessary towards a consistent treatment beyond the mean-field level [14].

5 Phase diagram

Lattice data for the QCD phase diagram exist up to relatively high temperatures, but extrapolations to non-zero chemical potential are still subject to large uncertainties. It is nonetheless instructive to explore the phase diagram as calculated in the PNJL model [11] in comparison with present lattice QCD results. In particular, questions

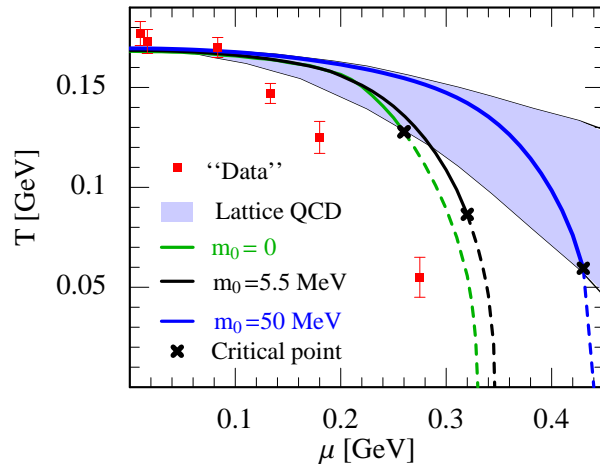


Figure 6: Phase diagram of the PNJL model for different values of the bare quark mass m_0 . Dashed lines correspond to a first order phase transition, full lines to a crossover. The band represents the extrapolation from lattice QCD results [22]. Also shown for orientation are the chemical freezeout “data” obtained through a thermal fit [23].

about the sensitivity of this phase diagram with respect to changes of the input quark masses will be addressed. This is an important issue, given the fact that most lattice QCD computations so far encounter technical limitations which restrict the input bare quark masses to relatively large values. The PNJL approach permits to vary the bare quark mass in a controlled way compatible with explicit chiral symmetry breaking in QCD. One can therefore interpolate between large quark masses presently accessible in lattice simulations, the physically relevant range of light quark masses around 5 MeV and further down to the chiral limit.

Fig. 6 presents our two-flavour PNJL results of the phase boundaries in the (T, μ) plane. These calculations should still be considered as an exploratory study since they do not yet include explicit diquark degrees of freedom, an important ingredient when turning to large chemical potentials, and the Polyakov loop fields are still treated in an approximate mean-field framework. Some interesting tendencies are, however, already apparent at the present stage.

Curves are shown for three different values of the bare quark mass. For $m_0 = 50$ MeV our result falls within the broad band of lattice extrapolations using an expansion in powers of the quark chemical potential. Reducing the bare quark mass toward physically realistic values leaves the phase diagram at small chemical potentials basically unchanged. However, the phase boundary is shifted quite significantly to lower temperatures at increasing chemical potentials when m_0 is lowered. Also shown in the figure is the position of the critical point separating crossover from first order phase transition. In fact, examining the chiral condensate and the Polyakov loop as functions of temperature for a broad range of chemical potentials (see Fig. 7), one

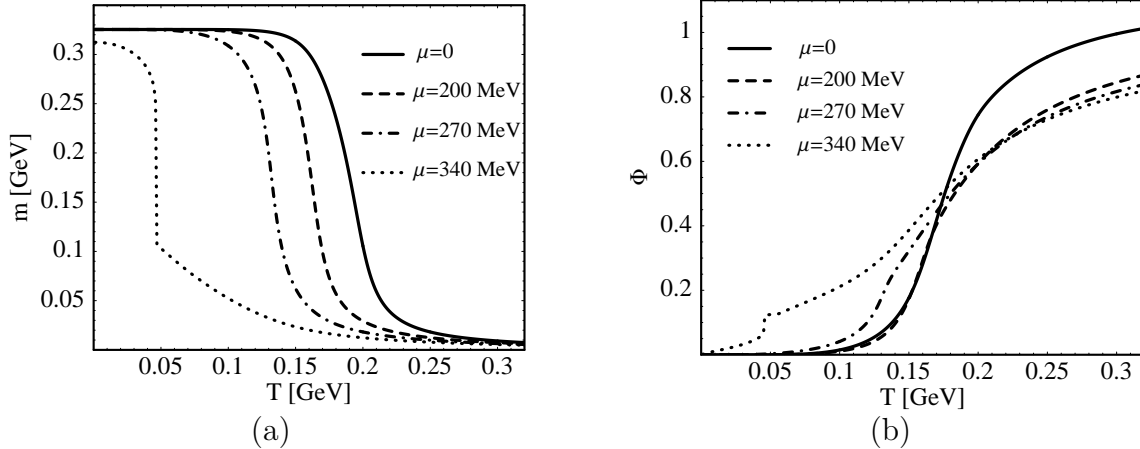


Figure 7: Constituent quark mass (a) and Polyakov loop (b) as functions of temperature for different values of the chemical potential. In both figures, $m_0 = 5.5$ MeV.

observes that there is a critical chemical potential above which these two quantities indicate a discontinuous jump from the confined (chirally broken) to the deconfined (chirally restored) phase. While a more precise location of this critical point is subject to further refined calculations [14], the qualitative features outlined here are expected to remain, such as the observation that the position of the critical point depends sensitively on the input quark mass.

6 Conclusions

The PNJL approach represents a minimal synthesis of the two basic principles that govern QCD at low temperatures: spontaneous chiral symmetry breaking and confinement. The respective order parameters (the chiral quark condensate and the Polyakov loop) are given the meaning of collective degrees of freedom. Quarks couple to these collective fields according to the symmetry rules dictated by QCD itself.

A limited set of input parameters is adjusted to reproduce lattice QCD results in the pure gauge sector and pion properties in the hadron sector. Then the quark-gluon thermodynamics above T_c up to about twice the critical temperature is well reproduced, including quark densities up to chemical potentials of about 0.2 GeV. In particular, the PNJL model correctly describes the step from the first-order deconfinement transition observed in pure-gauge lattice QCD (with $T_c \simeq 270$ MeV) to the crossover transition (with T_c around 200 MeV) when $N_f = 2$ light quark flavours are added. The non-trivial result is that the crossovers for chiral symmetry restoration and deconfinement almost coincide, as found in lattice simulations. The model also reproduces the quark number densities and pressure difference at various chemical potentials surprisingly well when confronted with corresponding lattice

data. Considering that the lattice results have been found by a Taylor expansion in powers of the chemical potential, this agreement indicates rapid convergence of the power series in μ .

The phase diagram predicted in this model has interesting implications. Starting from large quark masses an extrapolation to realistic small quark masses can be performed. The location of the critical point turns out to be sensitive to the input value of the bare (current) quark mass.

The conclusion to be drawn at this point is as follows. A quasiparticle approach, with its dynamics rooted in spontaneous chiral symmetry breaking and confinement and with parameters controlled by a few known properties of the gluonic and hadronic sectors of the QCD phase diagram, can account for essential observations from two-flavour $N_c = 3$ lattice QCD thermodynamics up to about twice the critical temperature of about 0.2 GeV. Presently ongoing further developments include:

- systematic steps beyond the mean-field approximation;
- extensions to 2+1 flavours;
- inclusion of explicit diquark degrees of freedom and investigations of colour superconductivity in the high density domain;
- detailed evaluations of susceptibilities and transport properties at finite chemical potential.

References

- [1] Y. Nambu and G. Jona-Lasinio, Phys. Rev. **122**, 345 (1961).
- [2] U. Vogl and W. Weise, Prog. Part. Nucl. Phys. **27**, 195 (1991).
- [3] S.P. Klevanski, Rev. Mod. Phys. **64**, 3 (1992).
- [4] T. Hatsuda and T. Kunihiro, Phys. Rep. **247**, 221 (1994).
- [5] G. Ripka, *Quarks Bound by Chiral Fields*, Clarendon, Oxford (1997).
- [6] M. Buballa, Phys. Rep. **407**, 205 (2005).
- [7] A. Barducci, R. Casalbuoni, G. Pettini and L. Ravagli, Phys. Rev. D **72**, 056002 (2005).
- [8] M. Alford, K. Rajagopal and F. Wilczek, Phys. Lett. **B422**, 247 (1998); R. Rapp, T. Schäfer, E.V. Shuryak and M. Velkovsky, Phys. Rev. Lett. **81**, 53 (1998).

- [9] A. Di Giacomo, H.G. Dosch, V.I. Shevchenko and Y.A. Simonov, Phys. Rep. **372**, 319 (2002).
- [10] C. Ratti and W. Weise, Phys. Rev. **D70**, 054013 (2004).
- [11] C. Ratti, M. A. Thaler and W. Weise, Phys. Rev. **D73**, 014019 (2006).
- [12] K. Fukushima, Phys. Lett. B **591**, 277 (2004).
- [13] A. Dumitru, R.D. Pisarski and D. Zschesche, Phys. Rev. **D72**, 065008 (2005).
- [14] S. Rößner, Diploma Thesis (2006); S. Rößner, C. Ratti and W. Weise, to be published.
- [15] P. N. Meisinger, M. C. Ogilvie and T. R. Miller, Phys. Lett. B **585**, 149 (2004).
- [16] G. Boyd *et al.*, Nucl. Phys. B **469**, 419 (1996).
- [17] O. Kaczmarek, F. Karsch, P. Petreczky, and F. Zantow, Phys. Lett. B **543**, 41 (2002).
- [18] F. Karsch, Lecture Notes in Phys. (Springer) **583**, 209 (2002);
F. Karsch, E. Laermann and A. Peikert, Nucl. Phys. B **605**, 579 (2002).
- [19] A. Ali Khan *et al.* Phys. Rev. D **64**, 074510 (2001).
- [20] C. R. Allton *et al.*, Phys. Rev. D **68**, 014507 (2003).
- [21] S.K. Ghosh, T.K. Mukherjee, M.G. Mustafa and R. Ray, hep-ph/0603050 (2006).
- [22] C. R. Allton *et al.*, Phys. Rev. D **66**, 074507 (2002).
- [23] A. Andronic and P. Braun-Munzinger, Lect. Notes Phys. **652**, 35 (2004).